doi: 10.4149/gpb_2014010

Ouabain modulation of snail Br neuron bursting activity after the exposure to 10 mT static magnetic field revealed by Higuchi fractal dimension

Srdjan Kesić[1], Ljiljana Nikolić[1], Aleksandar G. Savić[2], Branka Petković[1] and Sladjana Z. Spasić[2]

[1] *Department of Neurophysiology, Institute for Biological Research "Siniša Stanković", University of Belgrade, Despot Stefan Blvd. 142, 11060 Belgrade, Serbia*
[2] *Department for Life Sciences, Institute for Multidisciplinary Research, University of Belgrade, Kneza Višeslava 1, 11030 Belgrade, Serbia*

Abstract. Aim of this study was to investigate the application of normalized mean of the empirical Higuchi fractal dimension (*FD)* distributions, as a new approach to analyze the spontaneous bioelectrical activity of garden snail (*Helix pomatia)* Br neuron. The effect of ouabain on modulation of Br neuron bursting activity before and after the exposure to 10 mT static magnetic field (SMF) was observed by analyzing the following parameters: action potential (AP), interspike interval (ISI) and interbursting interval (IBI) components. Normalized mean of the empirical *FD* distributions were formed for the following experimental conditions: Control 1, Ouabain 1, Control 2, SMF 2, ASMF 2, Control 3, SMF 3 and Ouabain ASMF 3. Our main results have shown that ouabain without SMF induced increase in participation of AP and a decrease in participation of IBI components compared to the first control condition. However, in the presence of 10 mT SMF, ouabain-induced changes of measured parameters of Br neuron activity were less pronounced compared to the third control condition. We have shown that normalized mean of the empirical *FD* distributions is a useful method for detecting the changes in AP, ISI, and IBI components of complex bursting activity in altered physiological states.

Key words*:* Higuchi fractal dimension — Bursting activity — Ouabain — Na^+/K^+ pump — Static magnetic field

Abbreviations: AP, action potential; ASMF, after static magnetic field; *FD*, fractal dimension; IBI, interburst interval; ISI, interspike interval; SMF, static magnetic field.

Introduction

Higuchi fractal dimension measure alone, or as a preprocessing method in combination with other signal analysis techniques is very useful in the analysis of bursting activity and EEG signals that originate from neuronal networks (Goldberger et al. 2002; Spasic et al. 2008; Raghavendra and Narayana-Dutt 2010; Spasic et al. 2011a, b, c). As the biological signals are nonlinear by its nature, it was expected that nonlinear methods are more suitable for signal processing than classical linear techniques such as spectral and wavelet analysis (Goldberger et al. 2002). Higuchi fractal dimension allows fast computational analysis and characterization of various signal properties (Raghavendra and Narayana-Dutt 2010). By using fractal analysis it is possible to track changes in complexity of neuronal signals in normal and altered physiological states.

The bursting activity as a specific type of neuronal bioelectric activity can be associated with some of the most important physiological functions like respiration (Pena

Correspondence to: Sladjana Z. Spasić, Department of Life Sciences, Institute for Multidisciplinary Research, University of Belgrade, Kneza Višeslava 1, 11030 Belgrade, Serbia
E-mail: sladjana@imsi.rs, sladjana@imsi.bg.ac.rs, sladjana@ibiss.bg.ac.rs

2008) and heartbeat (Levy 1981). Bursting activity is the property of both, invertebrate and vertebrate neurons. In vertebrates, bursting activity can be found in structures such as neocortex (Le Bon-Jego and Yuste 2007), thalamus (Fuentealba and Steriade 2005), cerebellum (Raman et al. 2000) and neuroendocrine cells (Stojilkovic 2006). Bursting bioelectric activity consists of bursts of action potentials (AP) separated by interspike intervals (ISI) and interposed silent interburst periods (IBI) (Marsat and Pollack 2012). The spontaneously active Br neuron of the garden snail *(Helix pomatia*) subesophageal ganglion complex rhythmically generates bursts of AP separated by ISI and accompanied by silent IBI (Vadasz and Salanki 1976; Kononenko 2000). Single identified snail neurons, such as Br neuron, are a good experimental model because of their relatively large size, consistent position on the surface of the ganglia and consistent type of synaptic connections. All described properties of identified snail neurons make the experiments reproducible. Considering the role of bursting activity in the nervous systems of invertebrates and vertebrates including the human, it is very important to examine the bioelectric properties of these neurons in altered physiological states. External stimuli such as static magnetic field (SMF) or drug application can modulate normal bursting activity.

The sodium-potassium-activated adenosine triphosphatase (Na^+/K^+ pump or Na^+/K^+-ATPase) is responsible for establishing and maintaining resting membrane potential and it can be found in plasma membrane of all higher eukaryotes including snail neurons (Carpenter and Alving 1968; Gloor 1997). Electrochemical gradients of Na^+ and K^+ ions formed by Na^+/K^+ pump are necessary for maintenance and restoration of the resting membrane potential in excitable cells, Na^+-coupled transport of nutrients into cells and for osmotic balance (Rossier et al.1987). Increases in activity of Na^+/K^+ pump leads to membrane hyperpolarization, functioning as a negative feedback mechanism that protects the neurons against overexcitation (Munakata et al. 1998). Na^+/K^+ pump regulates the shape of AP in invertebrate and vertebrate neurons (Gadsby and Cranefield 1979; Pulver and Griffith 2010), and has an essential role in modulating bursting activity of identified snail Br neuron which displays bursting firing pattern (Nikolic et al. 2012). Furthermore, previous data showed that Na/K pump is involved in the modulation of Br neuron bursting activity by moderate intensity SMF of 10 mT (Nikolic et al. 2012).

Ouabain is a cardiac-glycoside that selectively acts on the extracellular face of the Na^+/K^+ pump and induces its inhibition. It leads to increase in intracellular levels of sodium ions consequently resulting in increased concentration of calcium ions (Prassas and Diamandis 2008). Ouabain can influence the strength of cardiac muscle contraction inducing positive inotropic effect (Koch-Weser and Blinks 1962). Micromolar to millimolar concentrations of glycoside ouabain inhibits the activity of Na^+/K^+ pump while the nanomolar concentrations of ouabain stimulates the activity of pump (Gao et al. 2002). Decreased activity of $Na^{+/}K^+$ pump plays an important role in pathogenesis of cardiovascular, neurological, renal and metabolic disorders (Rose and Valdes 1994).

Exploring the effects of magnetic field on living organisms at all levels of biological organization is very important. The significance is greater due to the use of different electrical devices in everyday life and modern medicine. Moderate-intensity magnetic fields (1 mT – 1 T) can influence the activity of some ion channels in cell membranes but the mechanisms of actions still remain unknown (Tolosa et al. 2011). Low frequency magnetic fields appear to increase charge movements within membrane protein, while electric fields during normal condition inhibited Na^+/K^+ pump activity (Blank 1995, 2005).

Previous research revealed increased activity of Na^+/K^+ pump during exposure to 10 mT SMF as revealed by measuring magnitude of ouabain's effect on parameters of neuronal electrical activity obtained by standard analysis such as membrane resting potential, frequency and duration of AP and ISI interval (Nikolic et al. 2012). In this study, we have used different nonlinear approaches in signal analysis and investigated the role of Na^+/K^+ pump in modulation of complexity of AP, ISI and IBI components of bursting activity of Br neuron during exposure to 10 mT SMF, measured as the magnitude of ouabain's effect.

The main objective of the present study was to investigate the possibility of using normalized mean of the empirical *FD* distribution as a fast and simple way to track changes in ouabain's modulation of bursting activity after the exposure to 10 mT SMF, which can be used complementary to classical signal analysis techniques.

Materials and Methods

Experimental procedure and data acquisition

All experiments were performed on Br neuron of the subesophageal ganglion complex of *H. pomatia* (*Pulmonata: Helicidae*). Details of isolation and dissection procedure of subesophageal ganglion complex are described in Nikolic et al. (2008). The position of Br neuron was established under the binocular microscope (Kerkut et al. 1975). Br neuron is positioned in the lower part of the right parietal ganglion. Under the binocular microscope it can be recognized according to its white color and relatively large size. Isolated brains were mounted in a Sylgard (Sylgard 184 Encapsulating Resin, Electronic materials Department Dow Corning Corporation, Midland, Michigan, USA) lined recording chamber containing circulating snail saline composed of 80 mM

NaCl, 5 mM $MgCl_2$, 10 mM $CaCl_2$, 4 mM KCl, and 5 mM Tris, pH 7.8. The permanent magnets, which produced SMF of 10 mT, were placed under the Petri dish of the recording chamber, with the North Pole orientated up, parallel to the vertical component of the geomagnetic field. The value of magnetic induction was measured directly on the surface of the subesophageal ganglion in the recording chamber by a GMO5 gaussmeter using a PT2837 probe (Hirsst, Magnetic Instruments Ltd, Cornwall, UK).

Voltage clamp (SEC-2 M, laboratory designed at Jozsef Atilla University, Szeged), two channel acquisition system MiniDigi 1A (Molecular devices, Sunnyvale, CA, USA) and AxoScope acquisition software (version 10.2, Axon Instruments, USA) were used for current clamp recordings and intracellular staining of Br neuron with Lucifer Yellow. Signals were sampled at 1 KHz and digitized using 16-bit A/D converter. To perform current clamp recordings and staining, Br neuron was impaled with glass microelectrode filled with 1 M K-citrate or 10–20% Lucifer Yellow CH (Molecular Probes) dissolved in distilled water (Schulze-Bonhage et al. 1993), respectively. Resistances of microelectrodes ranged from 10–20 MΩ. Lucifer Yellow was injected iontophoretically (Micro-Iontophoresis Programmer Model 160, World Precision Instruments, USA) in Br neuron soma by application of current pulses (3–5 nA, 5 Hz for 10–30 min). Br neuron stained with Lucifer Yellow was imaged with Zeiss Axiovert microscope (Zeiss, Austria).

The cardiac glycoside ouabain (10^{-4} M), an inhibitor of the Na^+/K^+ pump, was applied by gravity-driven bath perfusion to the recording chamber. Summary of the experimental design as well the effects of SMF and ouabain on neuronal Na^+/K^+ pump are presented on Fig. 1.

The experimental protocol for the first experimental group ($n = 4$) included following steps: perfusion of Br neurons with snail saline for 5 min (Control 1), followed by ouabain treatment for 7 min (Ouabain 1) with simultaneously current clamp recording. To exclude the possible contamination of prolonged action of SMF and to ensure that results of fractal analysis in ouabain ASMF (after static magnetic field) condition is a consequence of ouabain's effect, we included the second experimental group with 1 min recordings that includes ASMF period.

The second experimental group ($n = 5$) included recordings of Br neuron activity before (Control 2), during (SMF 2), and after the exposure to the static magnetic field of 10 mT (ASMF 2) for 15 min (Fig. 3A), according to the procedure thoroughly described in Nikolić et al. (2008).

The protocol for the third group SMF-exposed Br neurons ($n = 5$) was: perfusion of Br neurons with snail saline for 5 min (Control 3), exposure to 10 mT SMF for 15 min (SMF 3), and then treatment with ouabain for 7 min (Ouabain ASMF 3) with simultaneously recording. More details of experimental procedure are explained in references Nikolic et al. (2008, 2012). Schematic overviews of experimental protocols for the first, second and third group are presented in Fig. 2A, 3A, and 4A. A specification of the experimental groups is given in Table 1. For the fractal analysis we used only the last 1 min epochs of Control 1, Ouabain 1, Control 3, SMF 3 and Ouabain ASMF 3 conditions. For the

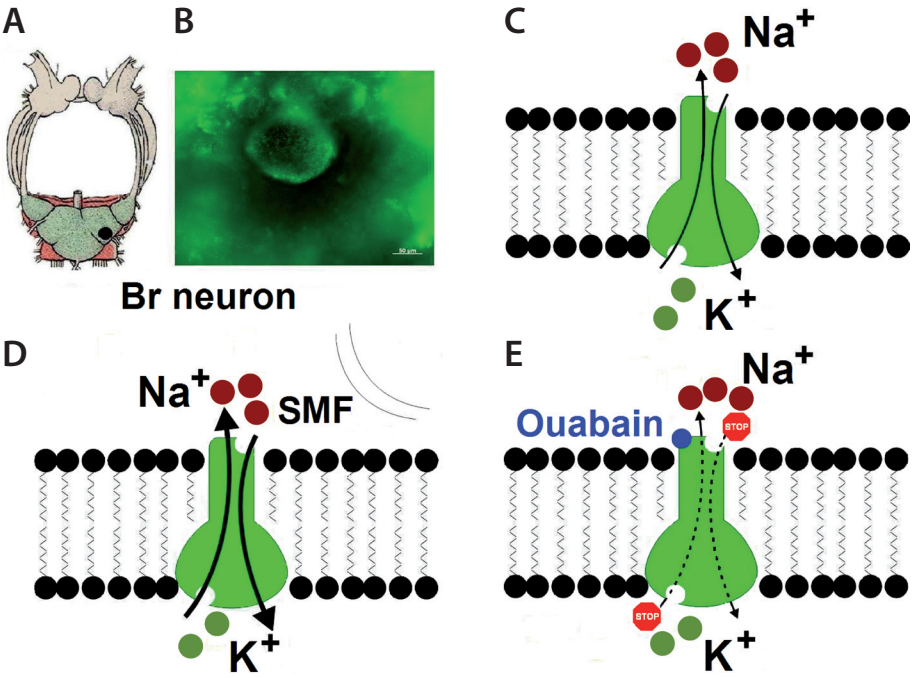

Figure 1. A. Position of Br neuron within subesophageal ganglia of *H. pomatia*. **B.** Br neuron stained with Lucifer Yellow. **C.** Simplified schematic outline of the Na^+/K^+ pump. **D.** Changes in the Na^+/K^+ pump functioning caused by short-term exposure to a moderate static magnetic field (SMF) , bolded arrows depicts increase in the Na^+/K^+ pump activity. **E.** The inhibitory effect of ouabain on neuronal Na^+/K^+ pump indicated by dashed arrows.

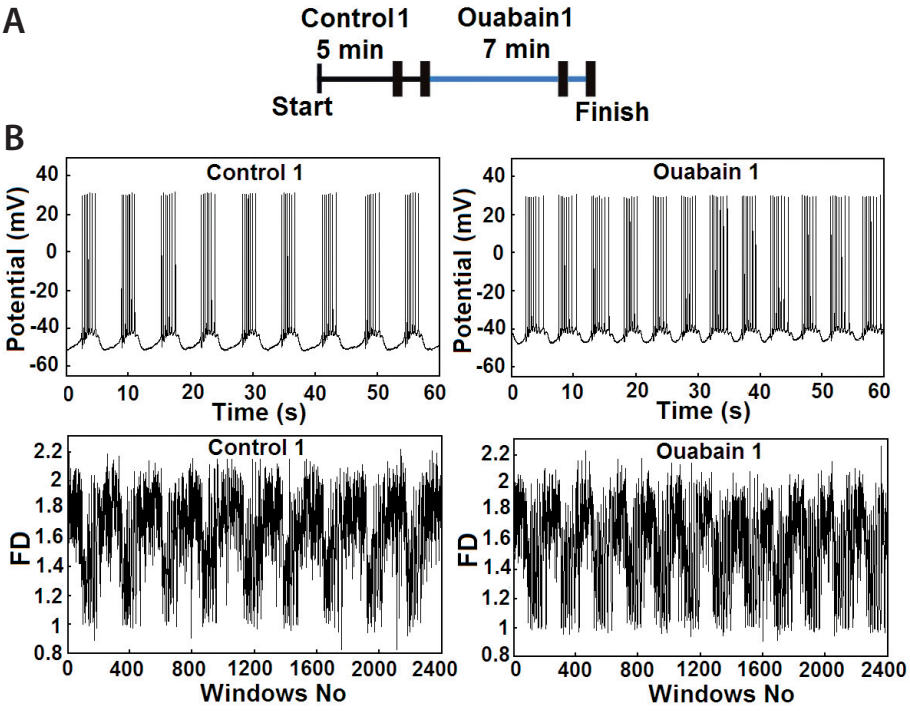

Figure 2. A. Time course of electrophysiological registration in control (Control 1) condition ($n = 4$) followed by ouabain (Ouabain 1) application ($n = 4$). Thick vertical lines denotes time period used for fractal analysis. **B.** Electrophysiological activity of garden snail (*H. pomatia*) Br neuron of subesophageal ganglion (60 s epochs) and corresponding fractal dimension (*FD*) values in control condition (left column) and after ouabain application (right column).

fractal analysis of second experimental group (Control 2, SMF 2, ASMF 2), we used the first 1 min epochs.

Fractal analysis – Higuchi fractal dimension and Normalized means of the empirical FD distributions

Higuchi's fractal dimension is a measure of geometrical signal complexity in time domain. Fractal analysis was performed by estimating the fractal dimension of electrophysiological signals (Fig. 2B, 3B, and 4B) from Br neurons using Higuchi's method (Higuchi 1988), based on self-developed script supported by MATLAB 6.5 (Spasic et al. 2008, 2011a, b, c; Spasic 2010). All details about the mathematical method are presented in reference Spasic et al. (2011a). Signals from spontaneously active Br neuron were analyzed in time sequences of 60 s with sampling frequency of 1 kHz. After preliminary tests, we chose the parameter $N = 25$ samples, that is equivalent to an epoch of 0.025 s duration because of non-stationary signals. The parameter k_{max} was equal to 8. Signals were divided into 12,000 epochs (windows). *FD* values were calculated for each epoch, without overlap. *FD* is the measure with theoretical values in the interval [1, 2]. In practice, Higuchi's fractal dimension may lie slightly outside the [1, 2] range, because it is only an estimate. The *FD* value of smooth curve should be estimated approximately 1 and the *FD* of random white noise is approximately 2.

Typical electrophysiological activity of Br neurons of subesophageal ganglion (60 s epochs) and corresponding fractal dimension values (in time domain) in Control 1, Ouabain 1, Control 2, SMF 2, ASMF 2, Control 3, SMF 3 and Ouabain ASMF 3 conditions are shown in Fig. 2B, 3B, and 4B.

Individual *FD* values were calculated and the empirical *FD* distributions for each individual signal were formed: 8 signals in Control 1 and Ouabain 1 condition from 4 snails, 15 signals for Control 2, SMF 2 and ASMF 2 conditions from 5 snails, and 15 signals for Control 3, SMF 3 and Ouabain ASMF 3 condition, obtained from 5 snails. Means of the empirical *FD* distributions for each experimental group were calculated. Additionally, normalization of mean empirical *FD* distribution was performed by dividing the frequencies for each group with its sum value (Fig. 5A, C, E). After normalization, curve fitting procedure was carried out in MATLAB 6.5 using cftool for all distributions with smoothing spline type of fit.

With the MATLAB Gaussian pick fitting procedure we established boundaries between *FD* values of AP, ISI, and IBI segments in the signal as it was described in reference Kesic et al. (2014). We separated each component of Br neuron bursting activity in normalized mean of the empirical *FD* distributions (boundaries are presented by dashed lines in Fig. 5A, C, E). Action potential is characterized by *FD* values in the interval of (0.8, 1.3], ISI with *FD* values in the interval (1.3, 1.75) and IBI component in the interval [1.75, 2.3). We calculated percentage participations (%) of AP, IS, IBI in normalized mean empirical *FD* distributions for all

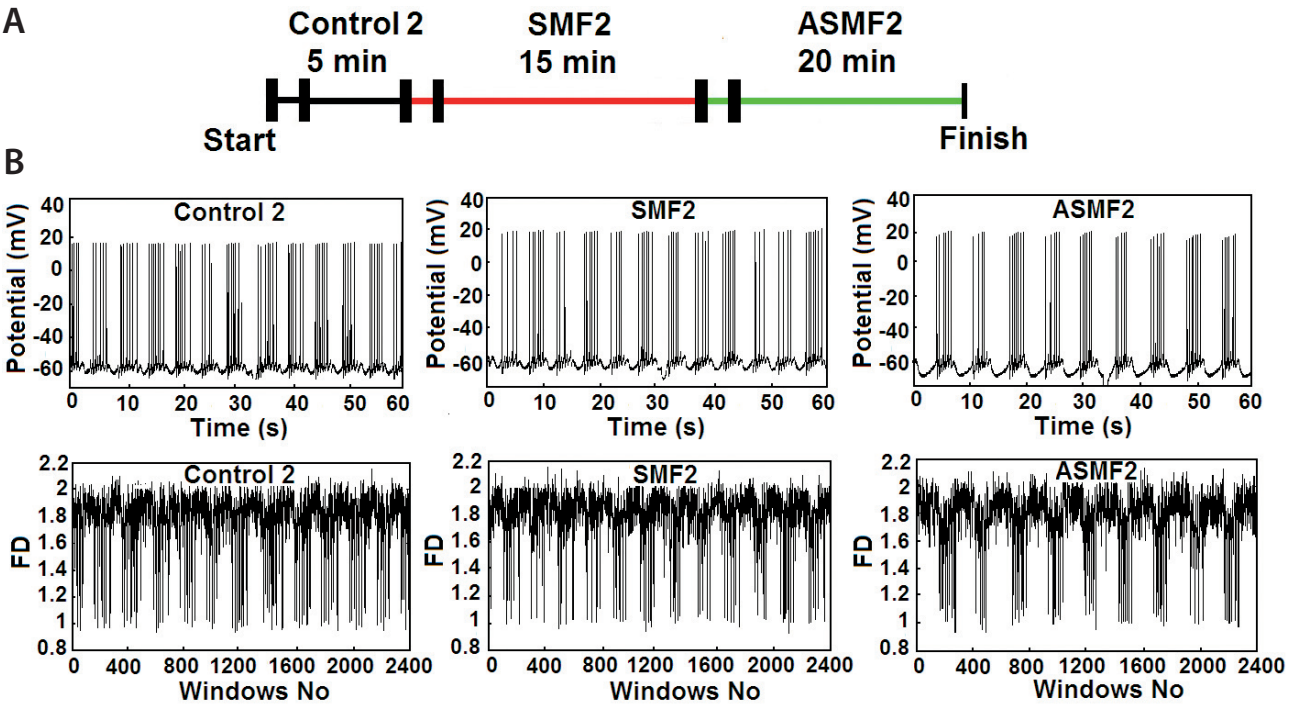

Figure 3. A. Time course of electrophysiological registration in control (Control 2) condition ($n = 5$), during SMF (SMF 2) exposure ($n = 5$) and in ASMF condition (ASMF 2) ($n = 5$). Thick vertical lines denotes time period used for fractal analysis. **B.** Typical electrophysiological activity of one garden snail (*H. pomatia*) Br neuron of subesophageal ganglion (60 s epochs) and corresponding fractal dimension (*FD*) values in control condition (left column), during SMF exposure (middle column) and in ASMF condition (right column).

experimental conditions by using cumulative distribution function.

Statistical analysis

The differences between the percentage participations of AP, ISI and IBI components in normalized mean of the empirical *FD* distributions within the first, second and third experimental groups were tested by nonparametric Friedman ANOVA and post hoc Wilcoxon Sign Ranks Test for two dependent samples using SPSS 13.0 software.

Results

Previous results published by Nikolic et al. (2012) showed that ouabain without SMF increased the duration of burst intervals, decreased the duration of interburst intervals, and increased the frequency of AP compared to the control condition. During the treatment with 10 mT SMF the duration of burst intervals decreased compared to the control condition. The duration of interburst intervals was not changed, while the frequency of AP decreased. In Ouabain ASMF condition, the duration of burst intervals was lower compared to the control condition, but higher compared to the SMF condition. The duration of interburst intervals was lower than in control and SMF conditions, while the frequency of AP was lower compared to the control and higher compared to the SMF conditions. Also, previous results indicated significant changes in the amplitude, frequency and the duration of the Br neuron action potential after treatment with 10 mT SMF. SMF of 10 mT decreased the AP frequency during exposure period (Nikolic et al. 2008).

Fitted normalized means of the empirical *FD* distributions for each experimental group with percentage participations of AP, ISI and IBI components are shown in Fig. 5 and Table 2.

The statistical analysis of the percentage participations of AP, ISI and IBI components with Wilcoxon test showed that there were differences between Control 1 *vs.* Ouabain 1 condition in AP ($Z = -5.418$, $p < 10^{-4}$), ISI ($Z = -5.841$, $p < 10^{-4}$) and IBI ($Z = -6.443$, $p < 10^{-4}$) components (Fig. 5A, B; Table 2). In the second experimental group there were differences in AP component between Control 2 *vs.* SMF 2 ($Z = -5.540$, $p < 10^{-4}$), Control 2 *vs.* ASMF 2 ($Z = -5.540$, $p < 10^{-4}$) and SMF 2 *vs.* ASMF 2 ($Z = -5.566$, $p < 10^{-4}$) and in ISI component between Control 2 *vs.* SMF 2 ($Z = -5.442$,

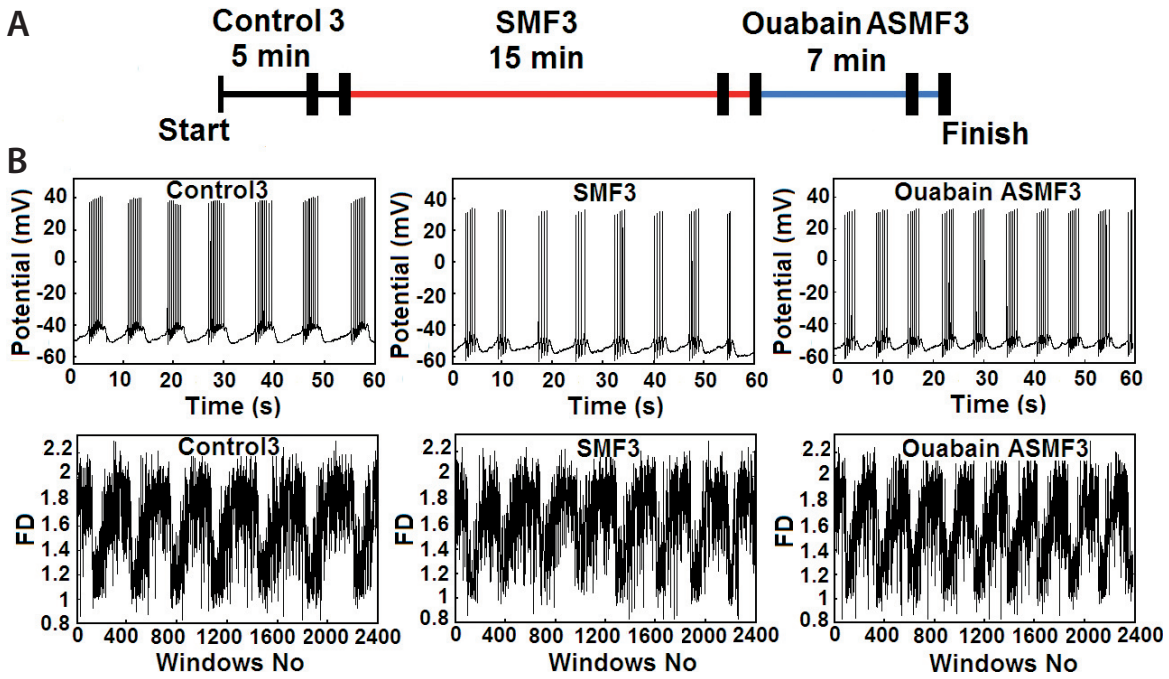

Figure 4. A. Time course of electrophysiological registration in control (Control 3) condition ($n = 5$), during SMF (SMF 3) exposure ($n = 5$) and in ouabain ASMF condition (Ouabain ASMF 3) ($n = 5$). Thick vertical lines denotes time period used for fractal analysis. **B.** Typical electrophysiological activity of one garden snail (*H. pomatia*) Br neuron of subesophageal ganglion (60 s epochs) and corresponding fractal dimension (*FD*) values in control condition (left column), during SMF exposure (middle column) and in ouabain ASMF condition (right column).

$p < 10^{-4}$), Control 2 *vs.* ASMF 2 ($Z = -4.549$, $p < 10^{-4}$), and SMF 2 *vs.* ASMF 2 ($Z = -2.093$, $p = 0.036$) (Fig. 5C, D; Table 2).

There were no differences between Control 2 *vs.* SMF 2 of IBI component ($Z = -0.401$, $p = 0.689$) but there were differences between Control 2 *vs.* ASMF 2 ($Z = -4.792$, $p < 10^{-4}$) and SMF 2 *vs.* ASMF 2 ($Z = -5.108$, $p < 10^{-4}$) (Fig. 5C, D; Table 2). There were significant differences in AP interval of the third experimental group between Control 3 *vs.* SMF 3 ($Z = -4.996$, $p < 10^{-4}$), Control 3 *vs.* Ouabain ASMF 3 ($Z = -6.215$, $p < 10^{-4}$) and SMF 3 *vs.* Ouabain ASMF 3 ($Z = -5.315$, $p < 10^{-4}$) as well as in ISI component of bursting activity between Control 3 *vs.* SMF 3 ($Z = -5.774$, $p < 10^{-4}$), Control 3 *vs.* Ouabain ASMF 3 ($Z = -5.841$, $p < 10^{-4}$) and SMF 3 *vs.* Ouabain ASMF 3 ($Z = -5.841$, $p < 10^{-4}$) and also in IBI component between Control 3 *vs.* SMF 3 ($Z = -5.806$, $p < 10^{-4}$), Control 3 *vs.* Ouabain ASMF 3 ($Z = -6.451$, $p < 10^{-4}$) and SMF 3 *vs.* Ouabain ASMF 3 ($Z = -6.433$, $p < 10^{-4}$) (Fig. 5E, F; Table 2).

Normalized mean of the empirical *FD* distribution analysis revealed that ouabain in the first experimental group increased participation of AP and ISI components at the expense of decreasing IBI component participation. In the second experimental group, compared to the control condition, SMF of 10 mT has reduced participation of AP and increased participation of ISI components while in ASMF period AP participation continues to decline with further increase of ISI participation and reduction of IBI. Within the third group, SMF of 10 mT reduced AP participation, increased ISI participation and decreased IBI participation compared to its control condition while ouabain ASMF increased AP, ISI and decreased IBI participation. Comparison

Table 1. A specification of the experimental conditions with number of experimental animals

I. experiment	Control 1 ($n = 4$)	–	Ouabain 1 ($n = 4$)	–
II. experiment	Control 2 ($n = 5$)	SMF 2 ($n = 5$)	–	ASMF 2 ($n = 5$)
III. experiment	Control 3 ($n = 5$)	SMF 3 ($n = 5$)	Ouabain ASMF 3 ($n = 5$)	

SMF, static magnetic field; ASMF, after static magnetic field.

between SMF 3 and Ouabain ASMF 3 showed significant increase in AP component at the expense of decrease in ISI and IBI components. As it can be seen that ouabain after applying SMF compared to the ouabain condition induced a smaller increase of AP and a smaller decrease of IBI component as a result of SMF action on bursting activity of Br neurons.

Discussion

Higuchi fractal dimension measure allows fast computational analysis of variations in signals. Calculation of *FD* by Higuchi's algorithm is very fast and simple and it has been often used alone or as a preprocessing technique in combination with other methods in signal analysis (Klonowski

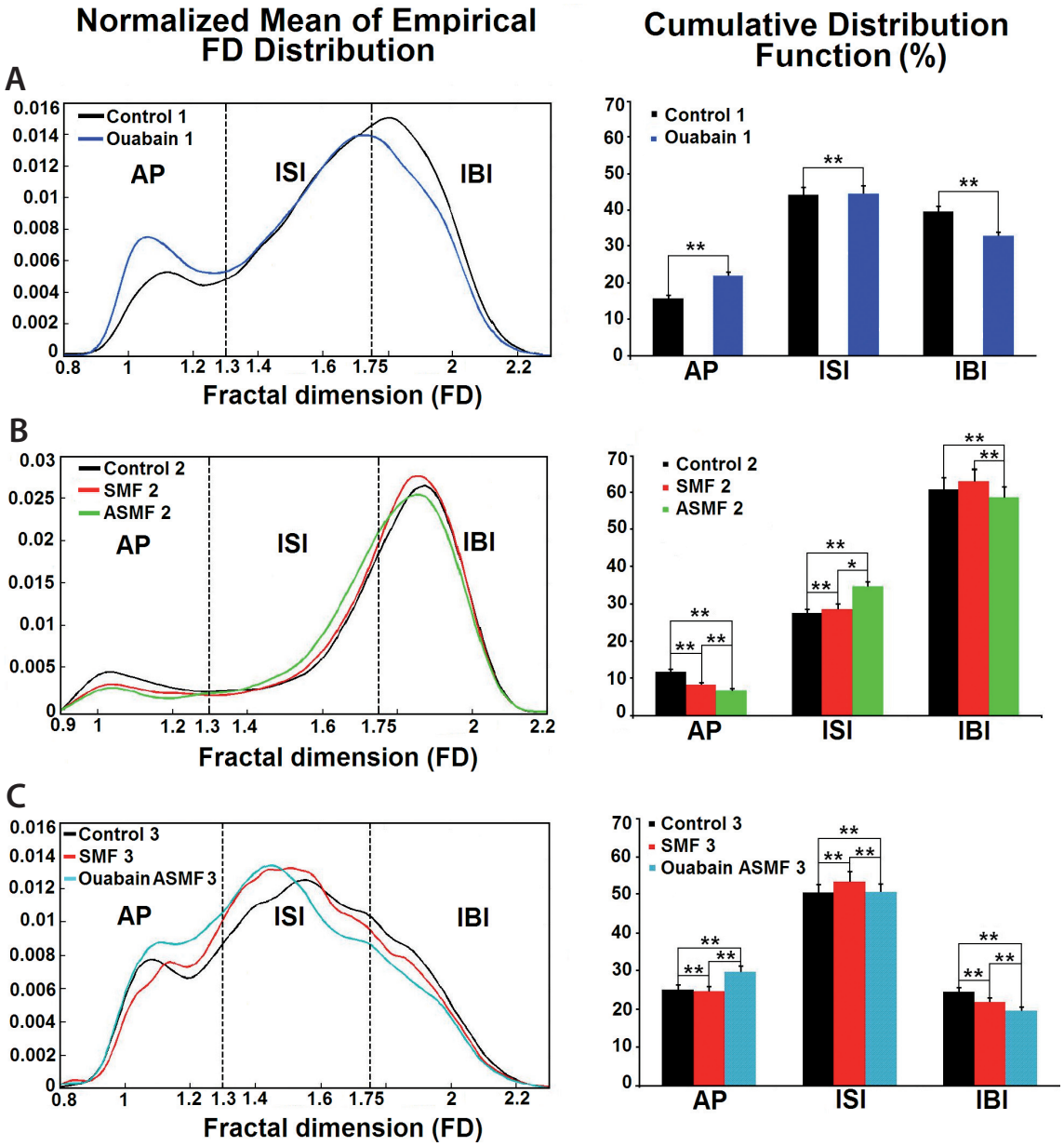

Figure 5. **A.** Normalized mean of empirical *FD* distribution of the first group in control (Control 1), and after ouabain application condition (Ouabain 1) with corresponding cumulative distribution function values. ** $p < 10^{-4}$ Ouabain 1 *vs.* Control 1. **B.** Normalized mean of empirical *FD* distribution in control (Control 2), during 10 mT SMF (SMF 2) and after static magnetic field exposure (ASMF 2) with corresponding CDF values. ** $p < 10^{-4}$ SMF 2 *vs.* Control 2, ASMF 2 *vs.* Control 2, SMF 2 *vs.* ASMF 2, * $p < 0.05$ SMF 2 *vs.* ASMF 2. **C.** Normalized mean of empirical *FD* distribution of the third group in control (Control 3), during 10 mT SMF (SMF 3), and after ouabain application (Ouabain ASMF 3) with corresponding CDF values. ** $p < 10^{-4}$ SMF 3 *vs.* Control 3, Ouabain ASMF 3 *vs.* Control 3, SMF 3 *vs.* Ouabain ASMF 3.

Table 2. Percentage participations of AP, IS, IBI in the mean group normalized empirical *FD* distributions

	AP (%)	ISI (%)	IBI (%)
Control 1	15.88	44.52	39.60
Ouabain 1	22.04	44.92	33.04
Control 2	11.69	27.35	60.96
SMF 2	8.14	28.71	63.15
ASMF 2	6.67	34.53	58.80
Control 3	25.06	50.41	24.53
SMF 3	24.61	53.47	21.92
Ouabain ASMF 3	29.73	50.53	19.74

AP, action potential; ISI, interspike interval; IBI, interburst interval; *FD*, fractal dimension; SMF, static magnetic field; ASMF, after static magnetic field.

et al. 2000; Spasic et al. 2008, 2011a, b, c; Raghavendra and Narayana-Dutt 2010). Accuracy of linear methods for signal analysis depends on stationarity of recorded signals (Spasic et al. 2008, 2011a; Klonowski 2009). For Higuchi's fractal analysis signal can be stationary, non-stationary, deterministic or stochastic (Klonowski et al. 2000; Spasic et al. 2008, 2011a; Klonowski 2009). Many processes within molluscan spontaneously active neurons are non-stationary, thus sometimes nonlinear methods of signal analysis have advantage in comparison to classical linear approaches (Schütt et al. 2002). However, combination of linear, nonlinear, and advanced statistical methods could be the best choice in revealing new fine details in complex biological and biomedical signal analysis.

In this paper using normalized mean of the empirical *FD* distribution allows us to further investigate the changes in the complexity of Br neuron activity after ouabain application with or without 10 mT SMF. By using this method we examined the changes in the complexity of Br neurons activity by measuring AP, ISI and IBI components.

Previous results showed that the effect of 10 mT SMF on Br neuron activity was mediated through the increased activity of Na^+/K^+ pump expressed as the magnitude of ouabain's effect measured on the membrane resting potential, AP and ISI duration (Nikolic et al. 2012). In this study by investigating the effect of ouabain with or without 10 mT SMF, we demonstrated use of normalized mean of empirical *FD* distribution as a sensitive, reliable, and fast method in revealing the changes in the complexity of AP, ISI, and IBI components induced by both 10 mT SMF and ouabain.

Ouabain and 10 mT SMF have opposite effects on the complexities of AP, ISI, and IBI components, which should be expected considering the fact that SMF increases while ouabain inhibits activity of Na^+/K^+ pump (Nikolic et al. 2012). Ouabain and ouabain after applied 10 mT SMF induce the same trend of changes in the percentage participations of AP, ISI, and IBI components compared to control condition. The changes in the percentage participations of the components of bursting activity in ASMF period were opposite to the changes observed during ouabain application with or without exposure to SMF. Thus, according to our data the effects of ouabain and ouabain ASMF on changes of signal's complexity were not consequences of post exposure influence of SMF on Br neuron activity.

It is well known that ouabain has a long history in the treatment of heart failure, in heart diseases such as angina pectoris and myocardial infarctions (Fürstenwerth 2010). Moderate intensity static magnetic fields can induce changes in functioning of nervous, cardiovascular and reproductive systems (Okano and Ohkubo 2005; Ye et al. 2008). Beside detrimental effects of electromagnetic radiation many studies point out the beneficial effects of the use of SMFs in medicine, from antinociceptive action to promotion of recovery of peripheral nerve injury, but the mechanism of action for achieving these effects is not completely known (Weintraub et al. 2003; Kelleher et al. 2006; Gyires et al. 2008). As many diseases are associated with decreased activity of Na^+/K^+ pump we could only speculate on the basis of our results that increased activity of pump mediated by 10 mT SMF could have a beneficial role. At this point we can't say that the altered bursting activity of Br neuron induced by ouabain application after the exposure to 10 mT SMF could be either hazardous or potentially beneficial, but evidently people with heart disease issues that use ouabain drugs should be aware of risks that arise in the presence of artificial sources of magnetic field in the environment.

Changes in bursting bioelectric activity may occur in nervous system of invertebrates and vertebrates exposed to magnetic field in similar manner. Thus, Azanza et al. (2000), has already proved that the behavior of snail (*H. aspera*) single neurons under exposure to SMFs (3 mT – 0.7 T) corresponds to mammal and human brain activity under magnetic field exposure (0.3 mT – 2.4 T).

Applied method could be useful in revealing the possible effects of static or alternating magnetic fields of different intensities alone or in combination with other chemical and physical stimuli that could modulate neuronal bursting activity. Except the bursting activity, normalized mean of empirical *FD* distribution method itself could be applied in analysis of activities of a single neuron and neuronal networks in physiological and pathological conditions.

Acknowledgements. This work was supported by projects 173027 and 173045 financed by The Serbian Ministry of Education, Science and Technological Development. All authors declare that they have no conflict of interest and no financial interest in the publication of this manuscript. The authors are especially grateful to the anonymous reviewers for their comments that help improve the manuscript.

References

Azanza M. J., Calvo A. C. (2000): Snail neuron bioelectric activity induced under static or sinusoidal magnetic fields reproduces mammal neuron responses under transcranial magnetic stimulation. Electromagnetic Biol. Med. **19,** 303–319 http://dx.doi.org/10.1081/JBC-100102121

Blank M. (1995): Biological effects of environmental electromagnetic fields: molecular mechanisms. BioSystems **35,** 175–178 http://dx.doi.org/10.1016/0303-2647(94)01509-6

Blank M. (2005): Do electromagnetic fields interact with electrons in the Na,K-ATPase? Bioelectromagnetics **26,** 677–683 http://dx.doi.org/10.1002/bem.20167

Carpenter D., Alving B. (1968): A contribution of an electrogenic Na+ pump to membrane potential in Aplysia neurons. J. Gen. Physiol. **52,** 1–21 http://dx.doi.org/10.1085/jgp.52.1.1

Fuentealba P., Steriade M. (2005): The reticular nucleus revisited: intrinsic and network properties of a thalamic pacemaker. Prog. Neurobiol. **75,** 125–141 http://dx.doi.org/10.1016/j.pneurobio.2005.01.002

Fürstenwerth H. (2010): Ouabain – the insulin of the heart. Int. J. Clin. Prac. **64,** 1591–1594 http://dx.doi.org/10.1111/j.1742-1241.2010.02395.x

Gadsby D., Cranefield P. (1979): Electrogenic sodium extrusion in cardiac Purkinje fibers. J. Gen. Physiol. **73,** 819–837 http://dx.doi.org/10.1085/jgp.73.6.819

Gao J., Wymore R. S., Wang Y., Gaudette G. R., Krukenkamp I. B., Cohen I. S., Mathias R. T. (2002): Isoform-specific stimulation of cardiac Na/K pumps by nanomolar concentrations of glycosides. J. Gen. Physiol. **119,** 297–312 http://dx.doi.org/10.1085/jgp.20028501

Gloor S. M. (1997): Relevance of Na,K-ATPase to local extracellular potassium homeostasis and modulation of synaptic transmission. FEBS Lett. **412,** 1–4 http://dx.doi.org/10.1016/S0014-5793(97)00774-6

Goldberger A. L., Amaral L. A., Hausdorff J. M., Ivanov P. Ch., Peng C. K., Stanley H. E. (2002): Fractal dynamics in physiology: Alterations with disease and aging. Proc. Natl. Acad. Sci. U.S.A. **99,** 2466–2472 http://dx.doi.org/10.1073/pnas.012579499

Gyires K., Zadori S. Z., Racz B., Laszlo J. (2008): Pharmacological analysis of inhomogeneous static magnetic field-induced antinociceptive action in the mouse. Bioelectromagnetics **29,** 456–462 http://dx.doi.org/10.1002/bem.20413

Higuchi T. (1988): Approach to an irregular time series on the basis of the fractal theory. Physica D. **31,** 277–283 http://dx.doi.org/10.1016/0167-2789(88)90081-4

Kelleher M. O., Al-Abri R. K., Lenihan D. V., Glasby M. A. (2006): Use of a static magnetic field to promote recovery after peripheral nerve injury. J. Neurosurg. **105,** 610–615 http://dx.doi.org/10.3171/jns.2006.105.4.610

Kerkut A., Lambert J., Gayton R. J., Loker E. J. (1975): Mapping of nerve cells in the subesophageal ganglia of Helix aspersa. Comp. Biochem. Physiol. 50A, 1–25 http://dx.doi.org/10.1016/S0010-406X(75)80194-0

Kesic S., Nikolic Lj., Janac B., Spasic S. (2014): Using Higuchi's Fractal Dimension in fine analysis of 2.7 mT and 10 mT static magnetic fields effects on the complex bursting activity of snail br neuron. Arch. Biol. Sci. (in press)

Klonowski W., Olejarczyk E., Stepien R. (2000): Nonlinear dynamics of EEG-signal reveals influence of magnetic field on the brain. IEEE **4,** 2955–2958

Klonowski W. (2009): Everything you wanted to ask about EEG but were afraid to get the right answer. Nonlinear Biomed. Phys. 3:2 http://dx.doi.org/10.1186/1753-4631-3-2

Koch-Weser J., Blinks J. R. (1962): Analysis of the relation of the positive inotropic action of cardiac glycosides to the frequency of contraction of heart muscle. J. Pharmacol. Exp. Ther. **136,** 305–317

Kononenko N. I. (2000): Role of the axodendritic tree in the functioning of Helix bursting neurons: generation of pacemaker activity and propagation of action potentials along the axon. Neuroscience **96,** 399–406 http://dx.doi.org/10.1016/S0306-4522(99)00543-6

Le Bon-Jego M., Yuste R. (2007): Persistently active, pacemaker-like neurons in neocortex. Front. Neurosci. **1,** 123–129 http://dx.doi.org/10.3389/neuro.01.1.1.009.2007

Levy M. N., Martin P. J., Stuesse S. L. (1981): Neural regulation of the heart beat. Annu. Rev. Physiol. **43,** 443–453 http://dx.doi.org/10.1146/annurev.ph.43.030181.002303

Marsat G., Pollack G. S. (2012): Bursting neurons and ultrasound avoidance in crickets. Front. Neurosci. 6–95

Munakata M., Fujimoto M., Jin Y. H., Akaike N. (1998): Characterization of electrogenic Na/K pump in rat neostriatal neurons. Brain Res. **800,** 282–293 http://dx.doi.org/10.1016/S0006-8993(98)00533-2

Nikolic Lj., Kartelija G., Nedeljković M. (2008): Effect of static magnetic fields on bioelectric properties of the Br and N-1 neurons of snail Helix pomatia. Comp. Biochem. Physiol. A Mol. Integr. Physiol.151, 657–663 http://dx.doi.org/10.1016/j.cbpa.2008.08.006

Nikolic Lj., Todorovic N., Zakrzewska J., Stanic M., Raus S., Kalauzi A., Janac B. (2012): Involvement of Na+/K+ pump in fine modulation of bursting activity of the snail Br neuron by 10 mT static magnetic field. J. Comp. Physiol. A.198, 525–540 http://dx.doi.org/10.1007/s00359-012-0727-0

Okano H., Ohkubo C. (2005): Effects of neck exposure to 5.5 mT static magnetic field on pharmacologically modulated blood pressure in conscious rabbits. Bioelectromagnetics **26,** 469–480 http://dx.doi.org/10.1002/bem.20115

Pena F. (2008): Contribution of pacemaker neurons to respiratory rhythms generation in vitro. Adv. Exp. Med. Biol. **605,** 114–118 http://dx.doi.org/10.1007/978-0-387-73693-8_20

Prassas I., Diamandis P. E. (2008): Novel therapeutic applications of cardiac glycosides. Nature Rev. Drug Discov. **7,** 926–935 http://dx.doi.org/10.1038/nrd2682

Pulver S. R., Griffith L. C. (2010): Spike integration and cellular memory in a rhythmic network from Na+/K+ pump current dynamics. Nat. Neurosci.13, 53–59 http://dx.doi.org/10.1038/nn.2444

Raghavendra B. S., Narayana-Dutt D. (2010): Signal characterization using fractal dimension, Fractals **18,** 287–292 http://dx.doi.org/10.1142/S0218348X10004968

Raman I. M., Gustafson A. E., Padgett D. (2000): Ionic currents and spontaneous firing in neurons isolated from the cerebellar nuclei. J. Neurosci. **20,** 9004–9016

Rose A. M., Valdes R. (1994): Understanding the sodium pump and its relevance to disease. Clin. Chem. **40,** 1674–1685

Rossier B. C., Geering K., Kraehenbuhl J. P. (1987): Regulation of the sodium pump: how and why? Trends Biochem. Sci.12, 483–487 http://dx.doi.org/10.1016/0968-0004(87)90235-0

Schulze-Bonhage A., Ulrich A., Speckmann E., Wittkowski W. (1993): Structure and Bioelectricity of single neurons of Helix pomatia in the intract nervous tissue during epileptic activity: simultaneous evaluations by confocal microscopy and intracellular recordings of membrane potential changes. Comp. Biochem. Physiol. A. **106,** 537–545 http://dx.doi.org/10.1016/0300-9629(93)90250-8

Schütt A., Rosso O. A., Figliola A. (2002): A discovery of new features of gastropod local field potentials by application of wavelet tools. J. Neurosci. Meth. **119,** 89–104 http://dx.doi.org/10.1016/S0165-0270(02)00184-X

Spasic S., Culic M., Grbic G., Martac Lj., Sekulic S., Mutavdzic D. (2008): Spectral and fractal analysis of cerebellar activity after single and repeated brain injury. Bull. Math. Biol. **70,** 1235–1249 http://dx.doi.org/10.1007/s11538-008-9306-5

Spasic S. (2010): Surrogate data test for nonlinearity of the rat cerebellar electrocorticogram in the model of brain injury. Signal Process **90,** 3015–3025 http://dx.doi.org/10.1016/j.sigpro.2010.04.005

Spasic S., Nikolic Lj., Mutavdzic D., Saponjic J. (2011a): Independent complexity patterns in single neuron activity induced by static magnetic field. Comput. Meth. Programs Biomed. **104,** 212–218 http://dx.doi.org/10.1016/j.cmpb.2011.07.006

Spasic S., Kesic S., Kalauzi A., Saponjic J. (2011b): Different anesthesia in rat induces distinct inter-structure brain dynamic detected by Higuchi fractal dimension. Fractals19, 113–123 http://dx.doi.org/10.1142/S0218348X1100521X

Spasic S., Kalauzi A., Kesic S., Obradovic M., Saponjic J. (2011c): Surrogate data modeling the relationship between high frequency amplitudes and Higuchi fractal dimension of EEG signals in anesthetized rats. J. Theor. Biol. **289,** 160–166 http://dx.doi.org/10.1016/j.jtbi.2011.

Stojilkovic S. (2006): Pituitary cell type-specific electrical activity, calcium signaling and secretion. Biol. Res. **39,** 403–423 http://dx.doi.org/10.4067/S0716-97602006000300004

Tolosa M.F., Bouzat C., Cravero W. R. (2011): Effects of static magnetic fields on nicotinic cholinergic receptor function. Bioelectromagnetics **32,** 434 –442 http://dx.doi.org/10.1002/bem.20657

Vadasz I., Salanki J. (1976): Mechanisms of spike and burst generation in the bimodal pacemaker RPal neuron of Helix pomatia L. In: Neurobiology of Invertebrates. (Ed. J. Salanki), pp. 371–381, Akademiai Kiado, Budapest

Weintraub M. I., Wolfe G. I., Barohn R. A., Cole S. P., Parry G. J., Hayat G., Cohen J. A., Page J. C., Bromberg M. B., Schwartz S. L. (2003): Static magnetic field therapy for symptomatic diabetic neuropathy: a randomized, double-blind, placebo-controlled trial. Arch. Phys. Med. Rehabil. **84,** 736–746 http://dx.doi.org/10.1016/S0003-9993(03)00106-0

Ye S. R., Yang J. W., Lee Y. T., Tsai L.Y. (2008): Static magnetic field expose enhances neurotransmission in crayfish nervous system. Int. J. Radiat. Biol. **84,** 561–567 http://dx.doi.org/10.1080/09553000802203622

Received: December 20, 2013
Final version accepted: February 10, 2014